UC San Diego
UC San Diego Previously Published Works

Title

Bioluminescent response of individual dinoflagellate cells to hydrodynamic stress measured with millisecond resolution in a microfluidic device.

Permalink

https://escholarship.org/uc/item/49m3z9fd

Journal

The Journal of Experimental Biology, 211(17)

ISSN

0022-0949

Authors

Latz, Michael I
Bovard, Michelle
VanDelinder, Virginia
et al.

Publication Date

2008-09-01

Peer reviewed

Bioluminescent response of individual dinoflagellate cells to hydrodynamic stress measured with millisecond resolution in a microfluidic device

Michael I. Latz[1],*, Michelle Bovard[1],†, Virginia VanDelinder[2],†, Enrico Segre[3], Jim Rohr[1,4] and Alex Groisman[2],*

[1]Scripps Institution of Oceanography, University of California San Diego, La Jolla, CA 92093-0202, USA, [2]Department of Physics, University of California San Diego, La Jolla, CA 92093, USA, [3]Department of Physics Services, Weizmann Institute of Science, Rehovot, 76100 Israel and [4]SPAWAR Systems Center San Diego, 53560 Hull Street, San Diego, CA 92152, USA

*Authors for correspondence (e-mails: mlatz@ucsd.edu; agroisman@ucsd.edu)
†These authors contributed equally to this work

SUMMARY

Dinoflagellate bioluminescence serves as a model system for examining mechanosensing by suspended motile unicellular organisms. The response latency, i.e. the delay time between the mechanical stimulus and luminescent response, provides information about the mechanotransduction and signaling process, and must be accurately known for dinoflagellate bioluminescence to be used as a flow visualization tool. This study used a novel microfluidic device to measure the response latency of a large number of individual dinoflagellates with a resolution of a few milliseconds. Suspended cells of several dinoflagellate species approximately 35 μm in diameter were directed through a 200 μm deep channel to a barrier with a 15 μm clearance impassable to the cells. Bioluminescence was stimulated when cells encountered the barrier and experienced an abrupt increase in hydrodynamic drag, and was imaged using high numerical aperture optics and a high-speed low-light video system. The average response latency for *Lingulodinium polyedrum* strain HJ was 15 ms (N>300 cells) at the three highest flow rates tested, with a minimum latency of 12 ms. Cells produced multiple flashes with an interval as short as 5 ms between individual flashes, suggesting that repeat stimulation involved a subset of the entire intracellular signaling pathway. The mean response latency for the dinoflagellates *Pyrodinium bahamense*, *Alexandrium monilatum* and older and newer isolates of *L. polyedrum* ranged from 15 to 22 ms, similar to the latencies previously determined for larger dinoflagellates with different morphologies, possibly reflecting optimization of dinoflagellate bioluminescence as a rapid anti-predation behavior.

Supplementary material available online at http://jeb.biologists.org/cgi/content/full/211/17/2865/DC1

Key words: bioluminescence, *Alexandrium*, dinoflagellate, flash, latency, *Lingulodinium*, microfluidic, *Pyrodinium*.

INTRODUCTION

All organisms and cells sense external stimuli and respond to changes in their environment. Sensing of mechanical stimuli serves in the detection of vibrations and sound, acceleration, gravity, proprioception, pressure and fluid flow. In multicellular organisms, the mechanosensory system usually involves sensory cells, a neural network, and effectors such as muscle. Each system component introduces a lag between application of the stimulus and the physiological response. This lag, known as the stimulus response latency, provides crucial information on the processing and functionality of the sensory system (Friedman and Priebe, 1998). It also provides a sensitive sublethal assay for determining how sensory systems are affected by environmental conditions (Preuss and Faber, 2003) and contaminants (Levin et al., 2003; Clotfelter and Rodriguez, 2006). Of ecological significance is the behavioral response latency, the delay between stimulus and behavioral response. Some rapid predator escape behaviors of aquatic animals involve very short response latencies of <30 ms (Wine and Krasne, 1972; Blaxter and Batty, 1985; Eaton et al., 1988; Zoran and Drewes, 1988; Hartline et al., 1999; Lenz and Hartline, 1999; Buskey et al., 2002; Buskey and Hartline, 2003; Preuss and Faber, 2003).

Mechanosensing also plays important roles for individual cells of multicellular organisms and for unicellular organisms. Endothelial cells attached to the walls of blood vessels are subjected to fluid shear stress due to blood flow (Frangos, 1993), causing a number of rapid and long-term physiological, morphological and gene expression changes (Reinhart, 1994; Gudi et al., 1996; Chien et al., 1998; Chen et al., 2001). Suspended unicellular organisms such as ciliates and some flagellates use escape jumps to avoid predator feeding currents (Jakobsen, 2001; Jakobsen, 2002), whereas luminescent dinoflagellates use light flashes to disrupt predator feeding behavior (Buskey et al., 1983; Buskey and Swift, 1983).

Dinoflagellate bioluminescence is a fascinating model system for mechanosensing. Dinoflagellates, the most common sources of bioluminescence in coastal waters (Staples, 1966; Tett, 1971), use light emission as an anti-predator strategy. The mechanical stimulus from predator contact is thought to cause cell deformation that activates the mechanotransduction pathway. The luminescent response has a 'flash bulb' effect, disrupting the feeding behavior of a predator (Buskey et al., 1983; Buskey and Swift, 1983; Buskey et al., 1985; Buskey and Swift, 1985) and leading to a decrease in grazing (Esaias and Curl, 1972; White, 1979). Bioluminescence can also act as a 'burglar alarm' to attract secondary predators, increasing the risk to the dinoflagellate grazer (Morin, 1983; Mensinger and Case, 1992; Abrahams and Townsend, 1993; Fleisher and Case, 1995). In addition to its role in predator–prey interactions,

dinoflagellate bioluminescence is also stimulated by flow stresses of different origins that have sufficient magnitude to cause cell deformation. This type of stimulation is most commonly associated with high shear flows that are created in boundary layers around swimming animals (Hobson, 1966; Rohr et al., 1998), in ship wakes (Rohr et al., 2002) and in breaking surface waves (Stokes et al., 2004), leading to spectacular displays of bioluminescence during periods of high cell abundance (Staples, 1966; Rohr et al., 1998; Latz and Rohr, 2005).

The bioluminescence of dinoflagellates is stimulated by the velocity gradient rather than absolute flow velocity (Latz and Rohr, 1999; Maldonado and Latz, 2007) and can thus serve as a reporter of local velocity gradients and hydrodynamic stresses, making it a unique tool for both field (Rohr et al., 1999; Rohr et al., 2002) and laboratory (Chen et al., 2003; Stokes et al., 2004) flow visualization. Based on laboratory studies using well-characterized flow fields (Latz et al., 1994; Latz and Rohr, 1999; Latz et al., 2004a; Latz et al., 2004b) a statistical model has recently been developed that predicts bioluminescence intensity as a function of shear stress level and cell concentration (Deane and Stokes, 2005). This model has been used to infer flow properties from bioluminescence intensity in flows not amenable to conventional measurements. Nevertheless, if dinoflagellates do not respond instantaneously to the stimulus, in high-speed flows the location where the flash response is observed can be substantially downstream of the location where a cell is stimulated by high local shear.

A delay between stimulation and light emission reflects the dynamics of mechanotransduction and of activation of cellular signaling pathways. High mechanical stress increases the fluidity of the dinoflagellate plasma membrane (Mallipattu et al., 2002), causing activation of GTP-binding proteins (Chen et al., 2007) and a calcium flux, mainly from the release of Ca^{2+} from intracellular stores (von Dassow and Latz, 2002). The calcium flux leads to the generation of an action potential at the tonoplast, the membrane surrounding the vacuole (Eckert, 1966; Widder and Case, 1981a), causing a proton flux from the vacuole to cytoplasm (Nawata and Sibaoka, 1979) and a decrease in cytoplamic pH. Acidification acts on scintillons, vesicles in close proximity with the vacuole that contain the chemicals involved in the luminescent reaction (Johnson et al., 1985; Nicolas et al., 1991). Low pH activates luciferase, inactive at physiological pH, which catalyzes the luminescent reaction (Hastings and Dunlap, 1986). In *Lingulodinium polyedrum*, low pH also dissociates the luciferin substrate from its binding protein (Fogel and Hastings, 1971) and makes it available for oxidation, leading to light emission. The response latency represents the total duration of all these signal transduction events.

Using individual restrained dinoflagellate cells impaled with an electrode, the response latency to mechanical stimuli was previously estimated at ~20 ms for the heterotrophic *Noctiluca scintillans* (Eckert, 1965b; Eckert and Sibaoka, 1968) and the autotrophic *Pyrocystis fusiformis* (Widder and Case, 1981a). These are large, non-motile, non-thecate species reaching dimensions up to 1 mm. For a flow speed of 2 m s^{-1}, a response latency of 20 ms corresponds to a downstream translation of 4 cm, a distance over which flow properties can change considerably. Statistically robust measurements of the response latency are needed for motile unrestrained dinoflagellates used for luminescent flow visualization and for correlating their bioluminescent flash responses with flow properties.

To measure the latency of response of dinoflagellates to hydrodynamic stresses with high resolution, a few basic experimental conditions must be met. First, the exposure of dinoflagellates to the stresses must occur over a time interval much shorter than the expected response latency, i.e. less than 5–10 ms, and the moment of exposure needs to be recorded with a high accuracy. Second, the light emitted by individual dinoflagellates needs to be measured with high temporal resolution. As the total number of photons emitted in one flash event is relatively small, it is important to collect the emitted light efficiently using high numerical aperture (NA) optics. Both conditions are difficult to meet using the conventional table-top flow setups. Hydrodynamic stress applied by starting a flow (e.g. by switching on rotation in a Couette flow system) is only established after a characteristic transient time $t=d^2/v$, where v is the fluid kinematic viscosity (10^{-6} m^2 s^{-1} for water at 20°C) and d is the characteristic size of the flow setup (e.g. the size of the annular gap for a Couette flow system). Even in the smallest flow setup used previously (von Dassow et al., 2005), the transient time was 400 ms, much longer than the estimated latency time. In addition, table-top setups are incompatible with the standard high-NA short working distance microscope objectives, and the light emitted by luminescent cells is usually collected rather inefficiently with low-NA long working distance optics.

To meet the basic experimental conditions, we performed the experiments using a novel microfluidic setup. Microfluidics involves the study and application of flow in various arrangements of microscopic channels. The advent of microfluidic systems has led to a growing number of biological applications in the areas of cell culture, flow cytometry, cellular biosensors, immunoassays, enzyme assays and cellular chemotaxis (Stone et al., 2004; El-Ali et al., 2005; Huh et al., 2005; deMello, 2006; Whitesides, 2006). Flows of liquids in microscopic channels are almost always laminar, linear and stable. Therefore hydrodynamics stresses in the flow can be controlled with high precision (e.g. kept constant over extended periods of time and quickly switched when needed) and reproduced with high accuracy. Microfluidic flows with controlled stresses have been applied to studies of the strength of adhesion of fibroblasts (Lu et al., 2004) and neutrophils (Gutierrez and Groisman, 2007) to a substrate, shear stress responses of endothelial cells (Song et al., 2005) and hepatocytes (Tanaka et al., 2006) attached to a substrate, deformation of erythrocytes under shear (Zhao et al., 2006), swimming of microorganisms (Marcos and Stocker, 2006), and the effect of transient hydrodynamic forces on cell lysis of microalgae (Hu et al., 2007).

The primary technical goal of our study was to test the feasibility of using microfluidic technology to apply well-defined mechanical stimuli to cells with a short inception time and to observe the responses of a large number of individual cells with millisecond resolution. The primary scientific objective was to obtain precise measurements of the response latency of mechanically stimulated bioluminescence from different species of motile dinoflagellates. To achieve these goals, we used a continuous flow in a microfluidic device with channels of two separate depths that created a barrier impenetrable to the dinoflagellates while allowing the flow to pass through. When individual cells were brought by the flow to the barrier, they came to a sudden stop and were exposed to an abrupt increase in hydrodynamic stress, with a transition time on the order of 1 ms, that triggered their bioluminescent response. The impulse associated with the impact did not play a significant role in triggering the bioluminescence. Immobilization of the dinoflagellates at the barrier greatly facilitated observation of their bioluminescence, which was measured with a temporal resolution as high as 4 ms. In this initial study, we focused on the response latency, flash duration, characteristic number of flashes per cell and the intervals between flashes, while other parameters such as the temporal pattern of flash intensity were not considered.

The main species investigated was *Lingulodinium polyedrum* (Stein) Dodge 1989, one of the most well-studied dinoflagellates in terms of general biology (Lewis and Hallett, 1997) and flow responses (Latz et al., 1994; Juhl et al., 2000; Juhl and Latz, 2002; Latz et al., 2004a; Latz et al., 2004b). *L. polyedrum* is a coastal species, 35 µm in diameter (Kamykowski et al., 1992), that is responsible for extensive blooms (Harrison, 1976; Gregorio and Pieper, 2000) with dramatic nighttime displays of bioluminescence (Latz and Rohr, 2005). The response latency was measured for three strains of *L. polyedrum*, an isolate of *Pyrodinium bahamense* Plate 1906 var. *bahamense* from a bioluminescent bay in Puerto Rico, and a Florida isolate of the saxitoxin-producing *Alexandrium monilatum* (Howell) Taylor 1979. The last two species are similar in size to *L. polyedrum*.

MATERIALS AND METHODS
Test organisms
The dinoflagellates tested are all motile thecate coastal species, approximately 35 µm in cell diameter. Three non-axenic, unialgal strains of *Lingulodinium polyedrum* (formerly *Gonyaulax polyedra*) collected from the Scripps Pier (La Jolla, CA, USA) were tested because the phenotype of a dinoflagellate, including its bioluminescence, can be affected by the time the dinoflagellate strain has been in culture (Sweeney, 1986; Shankle, 2001; von Dassow et al., 2005). Therefore, we measured the response latencies of newer and older strains of *L. polyedrum* isolated from the Scripps Pier: strain CCMP407, isolated in 1970 by B. Sweeney; strain HJ, also referred to as strain LpSIO95 (Jeong et al., 2005), isolation date unknown; and strain CCMP1932, isolated in 1998 by A. Shankle. The CCMP designation refers to strains maintained by the Provasoli-Guillard National Center for Culture of Marine Phytoplankton (http://ccmp.bigelow.org). Other dinoflagellates tested were a strain of *Alexandrium monilatum* isolated in 2000 from the Mississippi Sound, USA, by J. Rogers (Juhl, 2005), and *Pyrodinium bahamense* isolated in 2000 from Bahía Fosforescente, La Parguera, PR, USA by A. Juhl. *P. bahamense* and *A. monilatum* were grown in f/2 medium (Guillard and Ryther, 1962) minus silicate at a temperature of 26°C, whereas the *L. polyedrum* strains were grown in half-strength f/2 medium at 20°C. All cultures were grown on a 12 h:12 h light:dark cycle. Only cultures in mid-exponential growth phase, i.e. 5–20 days after inoculation, were used. Cell concentrations were determined from cell counts of defined volumes (usually 10 µl) in a multi-well slide under the microscope. Toward the end of the light phase, when dinoflagellate bioluminescence is not mechanically stimulable (Biggley et al., 1969), a sample from the desired culture at a concentration of 2000–15,000 cells ml^{-1} was loaded into a 60 ml plastic syringe that was covered with opaque material at the beginning of the dark phase.

Microfluidic apparatus
The microchannel device had two inlets, two outlets, and channels of two different depths, 15 and 200 µm (Fig. 1). It was made out of a lithographically micro-machined polydimethylsiloxane (PDMS) chip sealed with a no. 1.5 microscope cover glass, using a fabrication procedure described elsewhere (Simonnet and Groisman, 2005). Flow in the microchannels was driven by setting differences in hydrostatic pressure between the inlets and outlets of the device (Fig. 1) (Groisman et al., 2003). The dinoflagellate cell suspension and filtered seawater were kept in four 60 ml plastic syringes, which were held upright. The syringe with the cell suspension was connected to inlet 1, and the three syringes with filtered seawater were connected to inlet 2 and outlets 1 and 2 (Fig. 1). The syringe
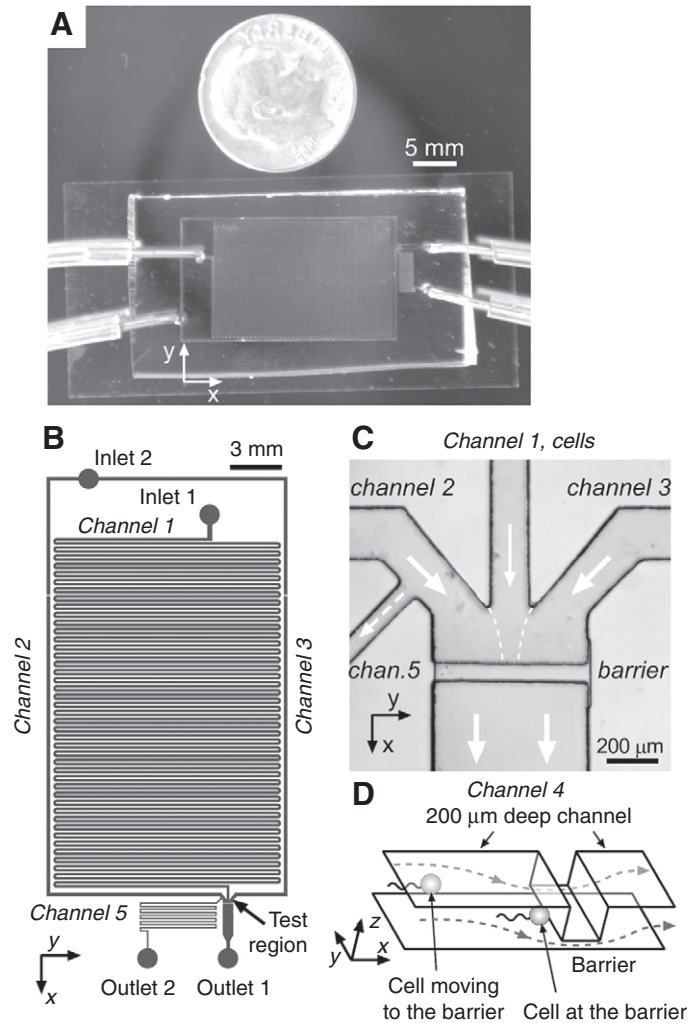
Fig. 1. The microfluidic device. (A) Microfluidic device and portion of connected tubing, shown with a dime for scale (17.91 mm in diameter). (B) Drawing of microchannels in the device. (C) Micrograph of test region, showing flow channels and barrier. Solid arrows indicate direction of flow in the device during its normal operation. Dashed arrow shows flow in channel 5 during the removal of cells from the barrier. Dashed lines mark the boundaries between streams from channels 2, 1 and 3. (D) Schematic three-dimensional drawing of barrier and cells (not to scale). Curved dashed lines are flow lines with arrows indicating flow direction. B and C are rotated 90 deg. counterclockwise with respect to A and D, as indicated by the orientation of the *x*- and *y*-axis shown in the panels.

linked to outlet 1 was connected through a solenoid valve to a source of compressed air with regulated pressure, P_g, which allowed the pressure at the outlet 1 to be increased by P_g for a pre-set amount of time.

The microfluidic device was designed to abruptly expose dinoflagellates to an adjustable level of mechanical stress and to create reproducible flow conditions for measuring the individual responses from large numbers of cells in repeated experiments. In the upstream part of the test region, channel 1, which is fed by inlet 1, merges with side channels 2 and 3, which are both fed by inlet 2 (Fig. 1C). The three merging channels form a single channel 4, which is 600 µm wide. Channels 1–3, as well as most of channel 4 have the same depth (h_0) of 200 µm. However, about 200 µm downstream from the merging, the depth of channel 4 (h_b) abruptly

decreased to 15 μm, creating a barrier that is impenetrable to the cells, which are approximately 35 μm in diameter (Fig. 1D). When the stream of the cell suspension from channel 1 enters channel 4, it is hydrodynamically focused between the streams of seawater from channels 2 and 3 and directed toward the center of the barrier. Observations showed that all dinoflagellates stopped at the entrance to the 15 μm deep section of channel 4 and rested in mechanical contact with both the barrier (wall in the *yz*-plane) and the bottom of the channel (wall in the *xy*-plane; Fig. 1D). Therefore, the drag force experienced by a cell at the barrier was largely independent of its original trajectory inside channels 1 and 4.

A cell passively flowing in a deep rectilinear channel, such as channel 1, moves with the average velocity of the liquid around it and thus experiences no net hydrodynamic drag. A mechanical stimulus applied to the cell originates from velocity gradients in the flow and the resulting shear stresses. When the cell arrives at the barrier, its motion stops and it is abruptly exposed to a hydrodynamic drag that originates from the flow of liquid around the stationary cell and is proportional to the characteristic velocity of this flow. The mean flow velocity under the barrier is a factor of $h_0/h_b \approx 13$ higher than the mean flow velocity in the channel 4. Therefore, the drag experienced by the cell at the barrier is particularly high and the arrival of the cells at the barrier triggers the bioluminescence response. The drag remains constant the entire time a cell stays at the barrier, eliciting multiple bioluminescent flashes by some cells (see below). An analysis of stimuli applied to a cell at the barrier and in a selected position upstream of the barrier is presented in the Numerical simulations subsections of Materials and Methods and Results.

The width of the cell-laden stream in channel 4 and at the barrier depends on the ratio of volumetric flow rates in channel 1 and channels 2 and 3, which is adjusted by varying pressures P_1 and P_2 at inlets 1 and 2, respectively. The width is normally three to five times smaller than the 150 μm width of channel 1, and the mean flow velocity in channel 1 is three to five times less than the velocity in channel 4. The resulting shear stress experienced by cells in channel 1 ($<0.3\,\mathrm{N\,m^{-2}}$) is lower than the luminescence response threshold for *L. polyedrum* (Latz et al., 1994; Latz and Rohr, 1999; Latz et al., 2004b) so the probability of premature stimulation of bioluminescence is minimal. Excessive reduction of the flow rate in channel 1 would be undesirable, however, because of the concomitant decrease in the number of cells reaching the test region per unit time. Channel 1 has a total length of 110 cm (Fig. 1B) and occupies most of the area of the microfluidic device. This long length is necessary to provide large flow resistance at low shear rate and to provide sufficient resolution when adjusting the rate of flow in channel 1 by varying P_1.

The flow in the device was steady, and cells were continuously arriving at the barrier. To prevent their accumulation at the barrier, which would alter the flow conditions, cells were removed from the test region a few seconds after their arrival by applying pressure P_g to outlet 1 for 1–3 s (Fig. 1B) causing cells to be evacuated through channel 5 towards outlet 2.

Numerical simulations

The goal of the numerical simulations was to evaluate forces acting on a dinoflagellate approaching and encountering the barrier. The domain of the simulations was a 150 μm long fragment of the 600 μm wide, 200 μm deep channel 4 immediately upstream of a 25 μm long fragment of the barrier (15 μm deep; see Fig. 2A). A dinoflagellate was modeled as a sphere with radius (R) of 17.5 μm. The model dinoflagellate was placed in the *xz*-plane of symmetry of the channel (Fig. 2A).
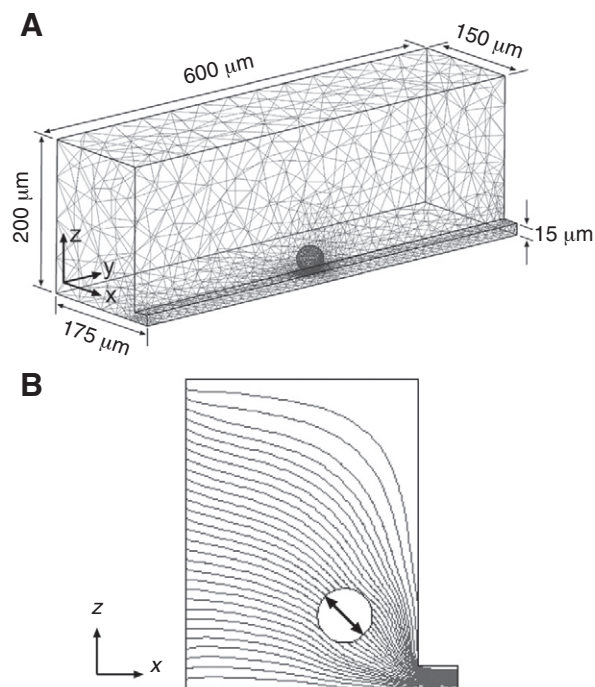

Fig. 2. Numerical simulations. (A) Three-dimensional schematic drawing of the segment of channel 4 used in the numeric simulations with a motionless sphere at the barrier. The mesh used in the simulations is shown by thin lines. (B) Two-dimensional cross-section of the channel in the *xz*-plane of symmetry (vertical midplane) with a freely moving sphere at (−30, 0, 30) μm from the rest position. Curved lines are the streamlines with the flow directed from left to right. Double-headed arrow shows the principal axis of tensile forces exerted at the sphere by the hydrodynamic stresses. Note the minimal bending of the streamlines in the vicinity of the sphere, as the sphere is moving together with the fluid.

The simulations were performed using the commercial finite element solver Comsol 3.2 (Femlab). Because of the curved boundary of the sphere representing the dinoflagellate, tetrahedral unstructured meshes were used and the mesh size was decreased in the vicinity of the sphere and of corners by the Comsol gridder. The boundary conditions were no slip on lateral walls (boundaries parallel to the *xy*- and *xz*-planes) and on the surface of the sphere. Different constant pressures were assigned to the entrance and the exit planes (boundaries parallel to the *yz*-plane), with the difference in the pressures driving the flow. The dynamic viscosity was taken to be $0.001\,\mathrm{kg\,m^{-1}\,s^{-1}}$ corresponding to seawater at 20°C (Vogel, 1981). The convergence and accuracy of the simulations was tested by comparing the results obtained with different mesh resolutions and gridding strategies. In addition, we verified that the *y*-component of the force and the *x* and *y* components of the torque applied by the flow to the sphere are close to zero.

The numerical simulations were performed for two different situations: with the sphere at the barrier and with the sphere approaching the barrier. In the former case, the sphere was assumed to be at rest, touching both the barrier and the lower boundary of the channel (Fig. 2A), and the total force exerted on the sphere by the flow was calculated. For the latter case, we took the sphere to be 30 μm in front of the barrier and 30 μm above the lower boundary of the channel (the center of the sphere at 47.5 μm in front of the barrier and 47.5 μm above the lower boundary). We calculated the translational and angular velocities of the sphere, assuming that the inertial forces were negligible compared with the viscous forces

and thus both the net force and net torque exerted on the sphere by the flow were zero. The computation was done iteratively. The translational and angular velocities of the sphere, $\mathbf{v}$ and $\boldsymbol{\omega}$, were assigned initial values of zero. At each iteration, the values of the force and torque, $\mathbf{F}$ and $\mathbf{T}$, exerted on the sphere by the flow were calculated, and $\mathbf{v}$ and $\boldsymbol{\omega}$ were updated according to $v^{(i+1)}=v^{(i)}-aF^{(i)}$ and $\omega^{(i+1)}=\omega^{(i)}-bT^{(i)}$ (where the upper index in the parentheses indicates the step number). The constants were chosen empirically at $a=10^9\,\mathrm{s\,kg^{-1}}$ and $b=10^{15}\,\mathrm{s\,m^{-2}\,kg^{-1}}$. The procedure was repeated 25 times until both $\mathbf{F}$ and $\mathbf{T}$ were essentially null ($F^{(25)}\sim10^{-3}F^{(0)}$ and $T^{(25)}\sim10^{-6}RF^{(0)}$), and the final values of $\mathbf{v}$ and $\boldsymbol{\omega}$ together with the flow velocity field after 25 iterations were used to calculate the forces applied to the sphere by the flow.

Imaging setup

The microfluidic device was mounted on the mechanical stage of a Zeiss Axiovert 135 inverted microscope (Carl Zeiss, Thornwood, NY, USA). To be able to record the arrival of dinoflagellates at the barrier, a low-level bright-field illumination was used. The test region was viewed using a $63\times/1.4$ or $40\times/0.75$ objective lens and a high-speed low-light video system consisting of a GENIISYS intensifier (DAGE-MTI of MC, Michigan City, IN, USA) coupled to an AVT Marlin F-033B digital video camera (Allied Vision Technologies GMBH, Stadtroda, Germany). The camera was computer-controlled *via* an IEEE 1394 interface with LabView IMAQ code (National Instruments Corporation, Austin, TX, USA). The images of the test region with luminescent cells were typically taken at a rate of $250\,\mathrm{frames\,s^{-1}}$ with a frame size of $96\times640\,\mathrm{pixels}$.

Data acquisition and analysis

A custom LabVIEW (National Instruments, Austin, TX, USA) virtual instrument (VI) provided control over video capture and camera parameters, such as frame rate, exposure time, and size of the region of interest. Video frames were collected in a 200–300 frame buffer; when a flash occurred, the buffer contents were saved to the computer hard drive. We used Vision Assistant 7.1 (National Instruments Corporation, Austin, TX, USA) to analyze the video sequences. To evaluate the latency in the bioluminescent response, the number of frames between the arrival of the cell at the barrier and the initiation of a flash was counted. The latency was calculated as the number of frames multiplied by the known interval between frames (the inverse of frame rate). For the video rate of $250\,\mathrm{frames\,s^{-1}}$, a three-frame delay resulted in an estimated response latency of $12\,\mathrm{ms}$ (see Fig. 3). The error associated with this method was caused by two uncertainties. One uncertainty was associated with the difference between the actual time of arrival of the cell at the barrier and the middle time point of the frame where the cell was first seen at the barrier. The other uncertainty was the difference between the actual beginning of the flash and the middle time point of the first frame with visible luminescence. Each of the uncertainties was estimated as a half of the interval between frames, and because the two uncertainties were independent from each other, the total error in the latency was estimated as 0.7 of the interval between frames, i.e. $3\,\mathrm{ms}$ for the frame rate of $250\,\mathrm{frames\,s^{-1}}$. To evaluate the duration of a flash, we counted the number of frames between the first frame with visible luminescence and the first frame where luminescence could not be seen any more. Finally, the interval between consecutive flashes was evaluated by counting the number of frames between the first frame with no luminescence (end of one flash) and the first frame with luminescence from the subsequent flash.

The flow velocity within the microfluidic device was measured using $1\,\mu\mathrm{m}$ diameter fluorescent beads (Bangs Laboratories, Inc., Fishers, IN, USA) as tracer particles. These measurements were done independently of the cell flashing experiments but under the same experimental conditions (driving pressures). The velocity of the beads was measured downstream of the barrier in channel 4 (Fig. 1C), where the flow channel dimensions were constant at $600\,\mu\mathrm{m}$ wide and $200\,\mu\mathrm{m}$ high. To evaluate the maximal flow velocity, v_{max}, we measured the length of the longest streaklines, corresponding to beads near the central axis of the channel. Knowing the maximum flow velocity and channel dimensions, the entire distribution as well as average flow velocity in the channel and volumetric flow rate can be calculated using the equations for fully developed laminar flow (White, 1991).

Values are expressed as mean $\pm$ s.d. unless otherwise stated. Statistical comparisons were done using Statview software (SAS Institute, Inc., Cary, NC, USA) and involved one-way analysis of variance (ANOVA) with *post-hoc* pairwise comparisons using Fisher's protected least significant difference (PLSD), or unpaired *t*-tests. Statistical significance was based on a P value of 0.05.

RESULTS
Numerical simulations

Numerical simulations were performed for maximum flow velocities, v_{max}, of 10, 20, and $40\,\mathrm{mm\,s^{-1}}$ in the $200\,\mu\mathrm{m}$ deep portion of channel 4. Because the characteristic Reynolds number (Re) in the flow, $Re=v_{max}h/\nu$, was always low ($Re\sim4$ at $v_{max}=20\,\mathrm{mm\,s^{-1}}$), a linear flow regime was expected. Indeed, the force exerted by the flow at the sphere at the barrier, F_b, was found to be proportional to v_{max}. The coefficient of proportionality between F_b and v_{max} was calculated to be $7.2\times10^{-6}\,\mathrm{kg\,s^{-1}}$, or $7.2\,\mathrm{nN\,mm^{-1}\,s}$ in more practical units, with a fractional error of 7%. The direction of the force was at 38° from the *x*-axis towards the bottom of the channel (–38° from the *x*-axis in the *xz*-plane). For example, for $v_{max}=20\,\mathrm{mm\,s^{-1}}$, the *x*-component, *z*-component, and absolute value of F_b were calculated to be $113\pm10\,\mathrm{nN}$, $-88\pm8\,\mathrm{nN}$, and $143\pm10\,\mathrm{nN}$, respectively. The force exerted at the sphere by the flow is balanced by the reaction and friction at the barrier and the bottom of the channel.

For the sphere at $\Delta x=30\,\mu\mathrm{m}$ in front of the barrier and $\Delta z=30\,\mu\mathrm{m}$ above the bottom of the channel (Fig. 2B) at $v_{max}=20\,\mathrm{mm\,s^{-1}}$, the two components of velocity of the sphere were $v_y=24.4\,\mathrm{mm\,s^{-1}}$ and $v_z=-22.2\,\mathrm{mm\,s^{-1}}$. The velocity was directed almost precisely along the bisector of the angle formed by the barrier and the bottom of the channel. Because of the symmetry of the flow with respect to the position of the sphere, we assumed that the principal axis of the tensile force exerted by the flow on the sphere was parallel to the direction of the motion of the sphere. To evaluate the tensile force, we numerically calculated the local force exerted by the moving liquid on different elements of the surface of the sphere and divided the sphere surface into two domains, with positive and negative projections of the local force onto the principal axis. The tensile force exerted on the sphere was calculated as a numeric integral of projections of the surface force onto the principal axis over the domain where the projections were positive. At $v_{max}=20\,\mathrm{mm\,s^{-1}}$ the tensile force was $F_a=3.0\,\mathrm{nN}$. A numeric integral over the domain with negative surface force was $-3.0\,\mathrm{nN}$, and the net force exerted by the flow on the sphere was zero, as imposed by the numeric simulation protocol.

When linearly extrapolated to $v_{max}=11\,\mathrm{mm\,s^{-1}}$ (a typical experimental value), the results of the simulations for a cell at $\Delta x=30\,\mu\mathrm{m}$ in front of the barrier give the force $F_a=1.6\,\mathrm{nN}$ and velocity $v_y=13.4\,\mathrm{mm\,s^{-1}}$ and $v_z=-12.2\,\mathrm{mm\,s^{-1}}$. For a cell at the barrier at the same flow conditions, the simulations predict a force
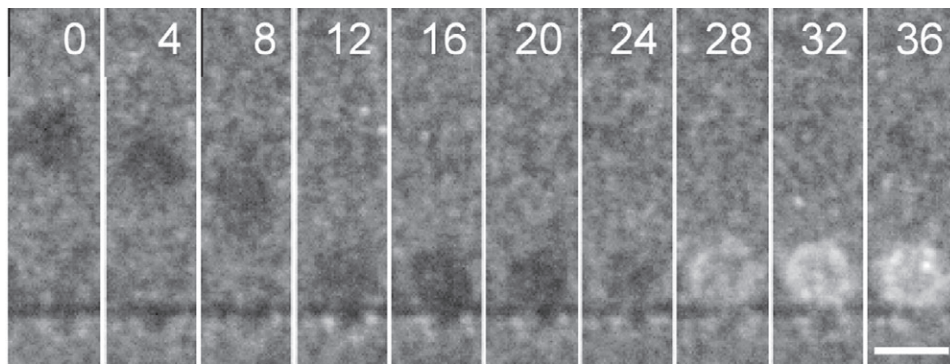
Fig. 3. Sequence of video frames of a single cell of *Lingulodinium polyedrum* strain HJ approaching the barrier (dark horizontal line near the bottom). Flow direction is from top to bottom. Frames were taken with an interval of 4 ms; the numbers at the top of each panel show elapsed time in milliseconds. The cell arrived at the barrier at 12 ms and the flash started at 24 ms, resulting in a latency of 12 ms. Scale bar, 50 μm.

F_b=79 nN. Because the sphere accelerates as it approaches the barrier, the time required for it to reach the barrier is less than $\Delta z/v_z$=2.5 ms. Therefore, the results of the simulations suggest that at the typical experimental conditions, the mechanical stimulus experienced by a dinoflagellate reaching the barrier increases about 48 fold (from F_a=1.6 nN to F_b=79 nN) within less than 2.5 ms. In the lowest flow rate experiment, which had a flow velocity v_{max}=5.7 mm s^{-1}, the hydrodynamic force at the barrier was calculated as F_b=40 nN.

Experimental results for *L. polyedrum* strain HJ

Bioluminescence in the test region was only observed when dinoflagellate cells encountered the barrier (Fig. 3; supplementary material movie 1). For the experiment with the lowest v_{max} of 5.7 mm s^{-1}, approximately half the cells encountering the barrier responded with a flash. For the cells that produced flashes at this v_{max}, a majority (65%) had a relatively fast response (latencies <60 ms) and a latency of 31.3±8.4 ms (Table 1; Fig. 4A). The remaining cells produced a relatively slow response, with a latency of 285.4±180.0 ms (N=44). At a higher flow rate (v_{max}=11 mm s^{-1}), most of the cells encountering the barrier produced a flash, and the fraction of the cells displaying fast responses (86%) was higher than at v_{max}=5.7 mm s^{-1} (Fig. 4B). The latency of the fast responding cells was 24.8±4.2 ms (Table 1) and slowly responding cells had a response latency of 257.0±80.7 ms (N=14).

In experiments with $v_{max} \geqslant$15 mm s^{-1}, all responses were fast and the distribution of response latencies was narrow (Fig. 4C).

For example, at v_{max}=35 mm s^{-1}, the response latency ranged from 12 to 21 ms, with an average of 15.2 ms (Table 1). There was no significant difference in response latency among experiments with three highest v_{max} of 15, 35 and 61 mm s^{-1} (ANOVA, $F_{2,329}$=0.939, P=0.392). For the pooled data, the response latency was 15.4±2.4 ms (N=332). The mean response latency was a decreasing function of the flow velocity with saturation at $v_{max} \geqslant$15 mm s^{-1} (Table 1; Fig. 5).

We also evaluated the minimum response latency, representing the most rapid response by a cell to the mechanical stimulus at each test condition (Table 1; Fig. 5). For experiments with $v_{max} \geqslant$15 mm s^{-1}, the minimum latency was 12 ms (i.e. three video frames at 250 frames s^{-1}). At lower flow speeds, the minimum latency increased, reaching 16 ms (i.e. four frames at 250 frames s^{-1}) at the lowest flow velocity of v_{max}=5.7 mm s^{-1}.

The duration of luminescent flashes following the encounter with the barrier varied with flow velocity (Table 1). Interestingly, there was no significant difference in the duration of the flashes at v_{max}=15, 35 and 61 mm s^{-1} (ANOVA, $F_{2,92}$=1.025, P=0.363), the range of velocities where the response latency was saturated at a low value (Table 1; Fig. 5). However, the flash durations for the pooled data at these three high velocities (70.6±18.9 ms; N=95) were significantly different (t-test, t_{364}=10.365, P<0.0001) from and 78% greater than those at the two lower velocities (39.9±26.5 ms; N=271 for the pooled data at v_{max}=5.7 and 11 mm s^{-1}). Thus, larger hydrodynamic drag on cells at the barrier generally resulted not only in shorter latencies but also in longer duration flashes.

Table 1. Summary of experimental results for initial flashes produced by different strains of dinoflagellates at different flow velocities

Flow velocity, v_{max} (mm s^{-1})	Response latency (ms)	Minimum latency (ms)	Flash duration (ms)
Lingulodinium polyedrum HJ			
5.7±0.9	31.3±8.4 (83)	16	41.0±33.0 (171)
11.2±0.8	24.8±4.2 (85)	16	38.0±9.8 (100)
15.1±1.4	15.2±2.5 (122)	13	69.0±15.0 (53)
35.0±5.0	15.6±2.6 (111)	12	72.0±24.0 (31)
60.5±3.4	15.3±2.3 (99)	12	77.0±18.0 (11)
L. polyedrum CCMP1932			
47.0±2.0	22.1±11.5 (144)	12	
L. polyedrum CCMP407			
35.0±5.0	15.2±4.6 (136)	8	
Pyrodinium bahamense			
39.0±4.0	22.3±4.8 (126)	16	
Alexandrium monilatum			
34.0±2.0	15.2±2.8 (133)	12	

Values of flow velocity are best estimates ± uncertainties of the measurements. Response latency is presented as mean ± s.d., with the number of analyzed flashes in parentheses. The uncertainty for the minimum latency is 3 ms. Flash duration of the first flash is only for cells responding with at least three flashes; values are mean ± s.d., with the number of analyzed flashes in parentheses.
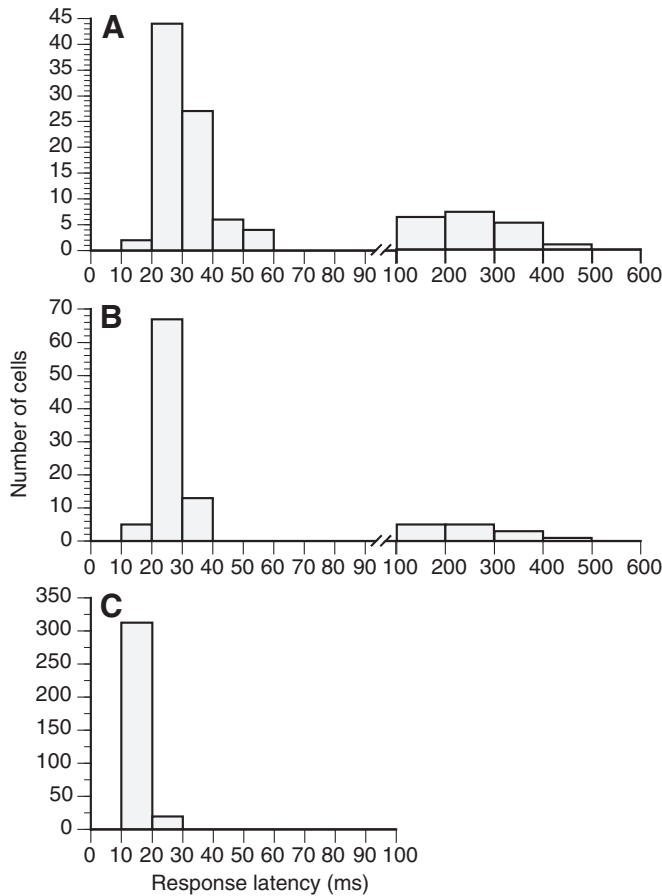
Fig. 4. Frequency distribution of response latency for *Lingulodinium polyedrum* strain HJ. (A) Response latency for the experiment with the lowest flow velocity of v_{max}=5.7 mm s⁻¹. (B) Response latency for the experiment with a flow velocity of v_{max}=11 mm s⁻¹. (C) Response latency for the experiments with the highest flow velocities (v_{max}=15, 35 and 61 mm s⁻¹). Bin width is 10 ms between 0 and 100 ms latency and 100 ms between 100 and 600 ms latency.
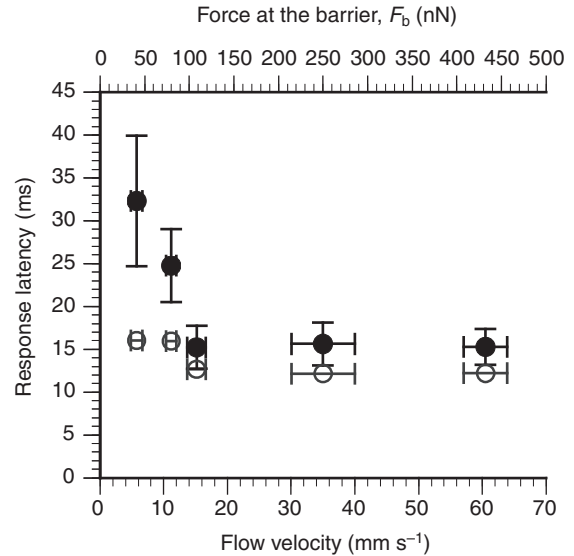

Fig. 5. Response latency of *Lingulodinium polyedrum* strain HJ as a function of flow velocity, v_{max}. Values represent the mean response latency (filled circles) and the minimum response latency (open circles). The *y*-axis error bars are s.d. of the response latencies, and the *x*-axis error bars are uncertainties of the flow velocity measurements.

Experimental results for other dinoflagellate strains

Measurements of the response latencies of newer and older strains of *L. polyedrum* isolated from the Scripps Pier were performed within the range of flow speeds (v_{max}⩾15 mm s⁻¹) where latency values for strain HJ were nearly constant. For the older strain CCMP407, isolated in 1970, the response latency at v_{max} of 35 mm s⁻¹ was 15.2±4.6 ms, while a newer strain CCMP1932, isolated in 1998, had a response latency of 22.1±11.5 ms for v_{max}=47 mm s⁻¹ (Table 1). There was a significant difference in response latency for the three strains (ANOVA, $F_{2,609}$=38.672, P<0.001) because the latency for strain CCMP1932 was significantly different (Fisher's PLSD, P<0.0001) and greater than the response latencies of strains HJ and CCMP407, which were not significantly different from each other (Fisher's PLSD, P=0.735). The minimum response latency was 12 ms for strains CCMP1932 and HJ, and 8 ms for strain CCMP407 (Table 1).

We also measured the response latencies of two other similarly sized thecate dinoflagellate species, *Pyrodinium bahamense* and *Alexandrium monilatum* (Table 1). The 22.3±4.8 ms response latency of *P. bahamense* was greater and significantly different (Fisher's PLSD, P<0.001) from the 15.2±2.8 ms latency of *A. monilatum* and that of *L. polyedrum* strains HJ and CCMP407 but was not significantly different from the latency of *L. polyedrum* strain CCMP1932 (P=0.883). The response latency of *A. monilatum* was not significantly different from those of *L. polyedrum* strains HJ and CCMP407 (P⩾0.846).

Multiple flashing

The response latencies and flash durations reported above were determined for the initial flash produced by cells after they encountered the barrier. Yet it is known that *L. polyedrum* and other dinoflagellates can produce more than one flash with mechanical stimulation (Widder and Case, 1981b; Latz and Lee, 1995; Latz and Jeong, 1996). In our microfluidic device many cells were observed to generate multiple luminescent flashes at the barrier. We investigated multiple flashing in detail for cells of *L. polyedrum* strain HJ, which flashed as many as four times within ~1 s after reaching the barrier. Flashes that might have occurred later were not registered, because our observation window was limited by the 300 frame buffer for video capture. Interestingly, the number of flashes produced by a cell at the barrier never exceeded two at the two highest flow velocities (v_{max}=35 and 61 mm s⁻¹; N=374), whereas the number of flashes reached four at the three lowest velocities (v_{max}=5.7, 11 and 15 mm s⁻¹; N=491 for the pooled data).

For cells that flashed three or four times (N=98 cells), the flash duration for pooled data was 43.8±13.2 ms (N=304). There was a significant variation in flash duration with flash number (Fig. 6A; ANOVA, $F_{3,300}$=17.169, P<0.0001). The duration of the first flash (36.7±8.7 ms; N=98) was significantly different from and smaller than that of the second to fourth flashes (47.3±13.6 ms; N=206), which were not significantly different from each other (Fisher's PLSD, P⩾0.156). There was a significant difference (t_{194}=5.829, P<0.0001) in the interval between 1st and 2nd flashes (117.5±52.1 ms; N=98) and that between the second and third flashes (65.8±70.5 ms; N=98; Fig. 6B). As only 11 out of 98 cells were observed to flash four times, the interval between the third and fourth flashes (83.8±33.0 ms) represented only a small subpopulation and was not used for statistical comparison. The minimum interval was
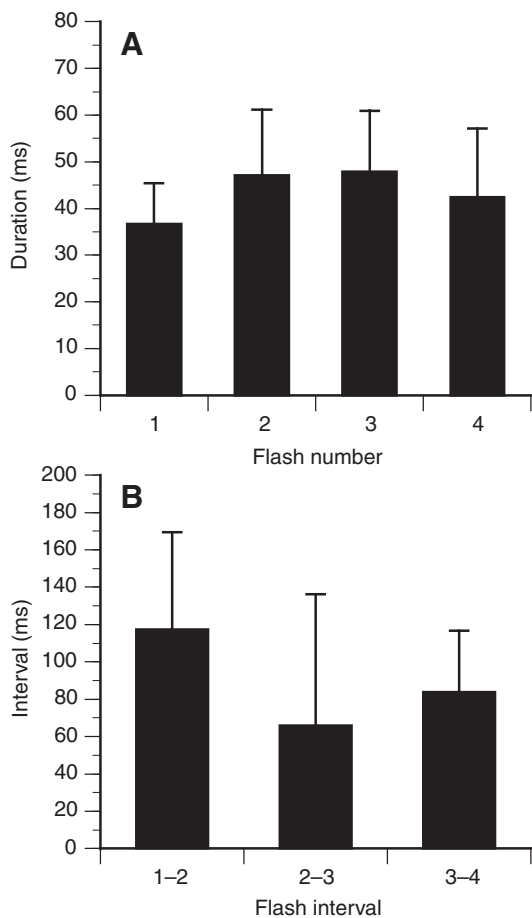
Fig. 6. Multiple flashes from individual cells of *Lingulodinium polyedrum* strain HJ. Data were collected for cells that flashed three or four times at v_{max}=5.7, 11 and 15 mm s^{-1}. (A) Duration of each flash as a function of flash number. Values are means ± s.d. (N=98 for flashes one to three; N=11 for flash four). (B) Length of interval between consecutive flashes. Values are means ± s.d. (N=98 for the intervals between the first and second and between the second and third flashes; N=11 for the interval between the third and fourth flashes).

4 ms between first and second flashes and 6 ms between second and third flashes.

DISCUSSION
Dinoflagellate response latency and cellular signaling pathway

The 15–22 ms response latency for dinoflagellate bioluminescence may be adaptive in terms of the ecological role of light emission as a predator defense to reduce the grazing rate of visual predators (Esaias and Curl, 1972; White, 1979) by altering their swimming to disrupt typical feeding behavior (Buskey et al., 1983; Buskey and Swift, 1983). Mechanical stimulation of bioluminescence appears to occur by direct predator contact (Latz et al., 2004b; von Dassow et al., 2005). Presumably a rapid response after contact with the predator increases the probability that a cell may escape from a predator prior to ingestion.

The characteristic response latencies measured for the tested dinoflagellates are similar to those of other aquatic organisms responding to mechanical stimuli in the context of predator avoidance. Minimum response latencies for rapid escape behaviors in aquatic organisms include 10–30 ms for fish startle escape behavior (Blaxter and Batty, 1985; Eaton et al., 1988; Preuss and Faber, 2003), 10 ms latency for crayfish responding to tactile stimuli (Wine and Krasne, 1972), 30 ms for the shadow response of copepods (Buskey and Hartline, 2003), and 7 ms for the tail withdrawal reflex of a polychaete (Zoran and Drewes, 1988). The 2–4 ms latency for copepod escape behaviors represents some of the most rapid responses (Hartline et al., 1999; Lenz and Hartline, 1999; Buskey et al., 2002). These rapid behavioral responses involve specialized neural networks including giant nerve fibers and myelinated nerves (Zoran and Drewes, 1988; Lenz et al., 2000; Weatherby et al., 2000).

The response latency in dinoflagellates reflects a complex series of cellular events triggered by mechanical stimulation. The timing of the individual steps of the signaling pathway was not resolved in our experiments. The timing is best understood for the large dinoflagellates *Noctiluca scintillans* and *Pyrocystis fusiformis* based on measurements of individual cells impaled by an electrode. In *N. scintillans* the overall response latency is 16–19 ms, with about a 15 ms delay between mechanical stimulation and the tonoplast action potential (Eckert and Sibaoka, 1968) and a 1–3 ms delay between the tonoplast action potential and initial light emission (Eckert, 1965b; Eckert, 1965a; Eckert, 1966). In *P. fusiformis* the overall response latency is about 17 ms, with a 5 ms delay between mechanical stimulation and the tonoplast action potential and a 12 ms delay between the action potential and the initial production of bioluminescence (Widder and Case, 1981a). The uncertainties in these values are not stated, so it is unknown to what extent the dissimilar timing for the two phases of the bioluminescence signaling pathway in *N. scintillans* and *P. fusiformis* is due to biological variability, methodological differences, or the unusual morphologies of these two non-thecate species (Eckert, 1966; Eckert and Sibaoka, 1968; Swift and Remsen, 1970; Seo and Fritz, 2000).

The morphologies of the species of dinoflagellates tested in our study are typical of thecate dinoflagellates (Netzel and Durr, 1984; Spector, 1984). It was expected that these smaller dinoflagellate species would have shorter latency times because of reduced diffusion distances of ions and a smaller surface area of the tonoplast membrane over which the action potential is propagated. However, their response latencies were similar to those of the larger species, perhaps reflecting the ecological value of dinoflagellate bioluminescence as a predator avoidance strategy. The minimum bioluminescence response latency is of interest because it represents the most rapid activity of the signaling pathways. CCMP407, the oldest strain of *L. polyedrum*, had the shortest minimum latency at 8 ms, while the other strains of *L. polyedrum*, as well as *A. monilatum*, had a minimum latency of 12 ms.

At low flow speeds the response latency of *L. polyedrum* HJ increased sharply. This response pattern is classically known for the electrical stimulation of neurons (Aidley, 1998) and is generally expected of a physiological response in that weaker stimuli will lead to a longer response latency. The pattern is consistent with the bioluminescence responses in fireflies (Buck et al., 1963), where bioluminescence is mediated through the nervous system and the response latency increases from 10 to 30 ms with decreasing strength of the electrical stimulus. This pattern also occurs with other classes of sensory stimuli, including hearing (Hoy, 1989; Stufflebeam et al., 1998) and vision (Aho et al., 1993).

Analysis of forces exerted on cells encountering the barrier

A dinoflagellate cell encountering the barrier experiences mechanical stimuli of two kinds. The stimulus of the first kind originates from the hydrodynamic drag on the immobilized cell that lasts as long as the cell stays at the barrier. As follows from the

numerical simulations, for v_{max}=11 mm s^{-1} the hydrodynamic drag amounts to a total force F_b=79 nN. The other stimulus is short term and originates from the impulse associated with impact. When a cell comes to a sudden stop at the barrier, there is an inertial force due to the change in momentum. The magnitude of the inertial force can be estimated as F_{in}=$p/\Delta t$, where p is the momentum of the cell, the product of its mass and velocity, and Δt is a characteristic time in which the velocity of the cell is reduced from its initial high value to zero. The mass, m, of a cell with a radius of 17.5 μm and density of 1084 kg m^{-3} (Kamykowski et al., 1992) is 2.4×10^{-11} kg, resulting in p=4.1×10^{-13} kg m s^{-1} or 4.1×10^{-4} nN s for a cell moving at v_c=17 mm s^{-1} (the absolute value of velocity calculated for Δx=30 μm and Δz=30 μm upstream from the barrier at v_{max}=11 mm s^{-1}). For this inertial force to be equal to the hydrodynamic drag, F_b, the impact has to last Δt=p/F_b=5 μs, corresponding to a distance Δx=$v_c\Delta t$=0.085 μm for a cell moving at v_c=17 mm s^{-1}.

When a cell comes close to the barrier, the liquid in a thin layer between the cell and the barrier is squeezed radially outwards at a high speed, producing large shear and a region of increased pressure between the cell and the barrier that results in a substantial resisting force (Brenner, 1961). To model the motion of a cell near the barrier, we again approximate the cell as a sphere with R=17.5 μm and approximate the barrier by an infinite surface in the yz-plane. It is a reasonable approximation, when the distance between the sphere and the barrier is substantially less than ~2.5 μm, the difference between R and the channel depth under the barrier. The resisting force experienced by the sphere moving at a speed v is inversely proportional to the distance from the barrier, x, and is given by F_r=$-6\pi R^2 v\mu/x$ (Brenner, 1961), where μ is the viscosity.

For v=v_c=17 mm s^{-1} and x=Δx=0.085 μm, we calculate the resisting force as F_r=1150 nN that is ~14 times greater that the hydrodynamic drag at the barrier, F_b=79 nN. Therefore, the resisting force near the barrier is expected to become comparable with F_b at distances, x, much greater than Δx=0.085 μm, resulting in the impact duration substantially larger than Δt=5 μs, and the impulse during the impact substantially smaller than the eventual drag force at the barrier, F_b. Because of the relatively low value of the impulse and short duration of the impact (still much less than 1 ms), the impulse associated with the impact is likely to be of relatively minor significance for the mechanical stimulation of the cells. This suggestion is supported by the observation of multiple flashing of cells immobilized at the barrier and exposed to a steady drag.

Minimum interval between repeated flashes *versus* minimum response latency

Dinoflagellates, including *L. polyedrum*, are known to produce more than one flash upon maintained mechanical stimulation (Widder and Case, 1981b; Latz and Lee, 1995; Latz and Jeong, 1996), but it has been assumed that the refractory period between repeated flashes would be long in comparison to the flash duration. For cells of *L. polyedrum* trapped at the barrier and experiencing steady hydrodynamic drag, the interval between first and second flashes was 117.5±52.1 ms and the interval between second and third flashes was 65.8±70.5 ms. Most surprisingly, the minimum interval between flashes was 4 ms, substantially less than the minimum response latency of 12 ms. We hypothesize that repeated flashing involves reactivation of only a subsystem of the entire mechanosensory signaling pathway. One possible candidate is the re-activation of the tonoplast action potential, which has a one-to-one association with a flash (Eckert, 1965a; Widder and Case, 1981a). Another possibility is that the rate of repeat flashing is limited by the need to restore physiological pH within the cell, because the proton-mediated tonoplast action potential leads to acidification of the cytoplasm, which activates the luminescent chemistry (Hastings and Dunlap, 1986; Wilson and Hastings, 1998). Thus cytoplasm pH must be restored to a physiological level, presumably by tonoplast membrane-associated ATPases that pump protons back into the vacuole.

Comparing mechanical simulation in the microfluidic device to previous flow experiments

To connect the results of this study with previous work on dinoflagellate bioluminescence in fully developed pipe flows, it is instructive to compare the stimuli experienced by a motionless cell at the barrier in the microfluidic device and by a moving cell experiencing shear in fully developed laminar pipe flow. Just as for a cell at the barrier, a cell in shear flow can be modeled as a sphere with radius R=17.5 μm, neglecting any active motion of the cell with respect to the flow. In this case, the net force on the cell is zero, and the cell can be divided into two hemispheres experiencing equal tensile forces, F=$(5/2)\pi R^2\gamma\mu$=$(5/2)\pi R^2\tau$, in opposing directions (Coufort and Line, 2003), where γ is the shear rate and τ is the shear stress in the flow. In previous studies, cell response was related to flow properties rather than forces acting on the cell. For example, in pipe flow *L. polyedrum* luminescence was first detectable in flows where the wall shear stress, τ_w, was about 0.3 N m^{-2} (Latz and Rohr, 1999); this level corresponds to a tensile force F=0.7 nN on each hemisphere of a cell. The fraction of flashing cells at the threshold was estimated as 0.0002 and it increased to 0.11 at τ=1 N m^{-2}, corresponding to a tensile force F=2.3 nN; the fraction remained at a level of ~0.1 up to the highest shear stress tested, ~20 N m^{-2}, corresponding to $F\approx50$ nN.

The mechanical stimuli applied to cells in our study were always substantially above the level at which the fraction of luminescent cells in the pipe flow reached the value of ~0.1 (Latz and Rohr, 1999). At the lowest tested flow velocity, v_{max}=5.7 mm s^{-1}, the estimated hydrodynamic force exerted on a cell at the barrier was F_b=40 nN. The fraction of flashing cells at these conditions was ~0.5, substantially higher than at the highest shear stress in pipe flow, and it further increased at higher v_{max} and F_b. The discrepancy in the fractions of flashing cells between the two experiments could be partly due to different observation conditions (imaging of quickly moving *versus* motionless cells). Furthermore, quantitative comparison between stimuli experienced by a stationary dinoflagellate at the barrier in the microfluidic device and one moving in shear flow is somewhat problematic, because of different distribution of hydrodynamic stress over the cell surface in these two situations. The application of relatively strong stimuli resulted in a high yield of luminescent cells and allowed us to observe the saturation in the response latency at $v_{max}\geqslant15$ mm s^{-1}. Thus, it was consistent with the objectives of this study to observe bioluminescent response of a large number of individual cells and to measure the minimal latency.

The response latency and luminescent flow visualization

Dinoflagellate bioluminescence is a useful flow visualization tool for conditions involving levels of shear stress above 0.1 N m^{-2}, such as the boundary layer flow on a moving dolphin (Rohr et al., 1998), high shear regions in bioreactors (Chen et al., 2003), and shear within a breaking wavecrest (Stokes et al., 2004). By developing a statistical model of the mechanical stimulation of dinoflagellate bioluminescence (Deane and Stokes, 2005), it can be used for quantitative estimates of shear or dissipation. Because high shears usually occur at high flow speeds, the response latency can lead to considerable downstream advection of organisms from

the points of their original stimulation before the luminescence starts. This effect is necessary to take into account this effect for reconstruction of the flow field from the distribution of bioluminescence. For example, in a nozzle flow with a speed of $2\,\mathrm{m\,s^{-1}}$ (Latz et al., 2004a), a response latency of $15\,\mathrm{ms}$ would result in distances as long as $3\,\mathrm{cm}$ between the regions of high shear where cells are stimulated and the regions where cell flashes are observed (Latz et al., 2004a). The information on dinoflagellate response latency obtained in this study can be incorporated into models relating dinoflagellate bioluminescence intensity to flow fields that cannot be measured using conventional techniques (Deane and Stokes, 2005).

Conclusions

The present work used a specially made microfluidic device to study the short-time dynamics of mechanosensing of motile dinoflagellates. A hydrodynamic drag was applied to individual cells with a millisecond inception time and the bioluminescence of the cells was recorded and used as a reporter of their response to this mechanical stimulus. The 15–22 ms response latencies observed with different strains of dinoflagellates are similar to those of other aquatic organisms to mechanical stimuli in the context of predator avoidance. This is intriguing because dinoflagellates are protists that appear to use a G-protein-mediated transduction system for mechanosensing. When stimulated continuously, cells often produced multiple flashes with intervals that were sometimes shorter than the initial response latency, suggesting that only a subset of the signal transduction pathway is involved in repeat flashing. Dinoflagellate bioluminescence could serve as a model system for understanding mechanosensing in simple eukaryotes, and the experimental techniques developed in this study could also be applied to studies of mechanosensing in different types of cells and in multicellular organisms.

LIST OF ABBREVIATIONS

d	characteristic size of the flow setup (e.g. the size of the annular gap for Couette flow)
Δt	duration of the impact needed for the impulse to be equal to the viscous drag
Δx	distance between sphere (or cell) and barrier along the flow direction
Δz	elevation of sphere (or cell) above bottom of channel
$\mathbf{F}$	force
F	magnitude of force
F_a	force acting on sphere $30\,\mu\mathrm{m}$ in front of the barrier
F_b	force acting on sphere at the barrier
F_in	inertial force
F_r	resistive force acting on sphere
γ	fluid shear rate
h	depth of microfluidic channel
μ	dynamic viscosity
ν	fluid kinematic viscosity ($10^{-6}\,\mathrm{m^2\,s^{-1}}$ for water at 20°C)
ω	magnitude of angular velocity
$\boldsymbol{\omega}$	angular velocity
p	momentum of the cell
P_g	regulated air pressure
P_1	pressure for inlet 1
P_2	pressure for inlet 2
R	radius of sphere or dinoflagellate cell
Re	Reynolds number
$\mathbf{T}$	torque
T	magnitude of torque
τ	fluid shear stress
$\mathbf{v}$	translational velocity
v_max	maximum flow velocity
v_x	x-component of velocity
v_y	y-component of velocity

REFERENCES

Abrahams, M. V. and Townsend, L. D. (1993). Bioluminescence in dinoflagellates: a test of the burglar alarm hypothesis. *Ecology* **258**, 260.

Aho, A. C., Donner, K., Helenius, S., Larsen, L. O. and Reuter, T. (1993). Visual performance of the toad (*Bufo bufo*) at low-light levels – retinal ganglion-cell responses and prey-catching accuracy. *J. Comp. Physiol. A* **172**, 671-682.

Aidley, D. J. (1998). *The Physiology of Excitable Cells* 4th ed. Cambridge: Cambridge University Press.

Biggley, W. H., Swift, E., Buchanan, R. J. and Seliger, H. H. (1969). Stimulable and spontaneous bioluminescence in the marine dinoflagellates, *Pyrodinium bahamense*, *Gonyaulax polyedra*, and *Pyrocystis lunula*. *J. Gen. Physiol.* **54**, 96-122.

Blaxter, J. H. S. and Batty, R. S. (1985). The development of startle responses in herring larvae. *J. Mar. Biolog. Assoc. UK* **65**, 737-750.

Brenner, H. (1961). The slow motion of a sphere through a viscous fluid towards a plane surface. *Chem. Eng. Sci.* **16**, 242-251.

Buck, J., Case, J. F. and Hanson, F. E., Jr (1963). Control of flashing in fireflies. III. Peripheral excitation. *Biol. Bull.* **125**, 251-269.

Buskey, E., Mills, L. and Swift, E. (1983). The effects of dinoflagellate bioluminescence on the swimming behavior of a marine copepod. *Limnol. Oceanogr.* **28**, 575-579.

Buskey, E. J. and Hartline, D. K. (2003). High-speed video analysis of the escape responses of the copepod *Acartia tonsa* to shadows. *Biol. Bull.* **204**, 28-37.

Buskey, E. J. and Swift, E. (1983). Behavioral responses of the coastal copepod *Acartia hudsonica* (Pinhey) to stimulated dinoflagellate bioluminescence. *J. Exp. Mar. Biol. Ecol.* **72**, 43-58.

Buskey, E. J. and Swift, E. (1985). Behavioral responses of oceanic zooplankton to simulated bioluminescence. *Biol. Bull.* **168**, 263-275.

Buskey, E. J., Reynolds, G. T., Swift, E. and Walton, A. J. (1985). Interactions between copepods and bioluminescent dinoflagellates: direct observations using image intensification. *Biol. Bull.* **169**, 530.

Buskey, E. J., Lenz, P. H. and Hartline, D. K. (2002). Escape behavior of planktonic copepods in response to hydrodynamic disturbances: high speed video analysis. *Mar. Ecol. Prog. Ser.* **235**, 135-146.

Chen, A. K., Latz, M. I. and Frangos, J. A. (2003). The use of dinoflagellate bioluminescence to characterize cell stimulation in bioreactors. *Biotechnol. Bioeng.* **83**, 93-103.

Chen, A. K., Latz, M. I., Sobolewski, P. and Frangos, J. A. (2007). Evidence for the role of G-proteins in flow stimulation of dinoflagellate bioluminescence. *Am. J. Physiol. Regul. Integr. Comp. Physiol.* **292**, R2020-R2027.

Chen, B. P. C., Li, Y. S., Zhao, Y. H., Chen, K. D., Li, S., Lao, J. M., Yuan, S. L., Shyy, J. Y. J. and Chien, S. (2001). DNA microarray analysis of gene expression in endothelial cells in response to 24-h shear stress. *Physiol. Genomics* **7**, 55-63.

Chien, S., Li, S. and Shyy, Y.-J. J. (1998). Effects of mechanical forces on signal transduction and gene expression in endothelial cells. *Hypertension* **31**, 162-169.

Clotfelter, E. D. and Rodriguez, A. C. (2006). Behavioral changes in fish exposed to phytoestrogens. *Environ. Pollut.* **144**, 833.

Coufort, C. and Line, A. (2003). Forces on spherical particles in terms of upstream flow characteristics. *Chem. Eng. Res. Des.* **81**, 1206-1211.

Deane, G. B. and Stokes, M. D. (2005). A quantitative model for flow-induced bioluminescence in dinoflagellates. *J. Theor. Biol.* **237**, 147-169.

deMello, A. J. (2006). Control and detection of chemical reactions in microfluidic systems. *Nature* **442**, 394-402.

Eaton, R. C., Didomenico, R. and Nissanov, J. (1988). Flexible body dynamics of the goldfish C-start: implications for reticulospinal command mechanisms. *J. Neurosci.* **8**, 2758-2768.

Eckert, R. (1965a). Bioelectric control of bioluminescence in the dinoflagellate *Noctiluca*. I. Specific nature of triggering events. *Science* **147**, 1140-1142.

Eckert, R. (1965b). Bioelectric control of bioluminescence in the dinoflagellate *Noctiluca*. II. Asynchronous flash initiation by a propagated triggering potential. *Science* **147**, 1142-1145.

Eckert, R. (1966). Excitation and luminescence in *Noctiluca miliaris*. In *Bioluminescence in Progress* (ed. F. H. Johnson and Y. Haneda), pp. 269-300. Princeton, NJ: Princeton University Press.

Eckert, R. and Sibaoka, T. (1968). The flash-triggering action potential of the luminescent dinoflagellate *Noctiluca*. *J. Gen. Physiol.* **52**, 258-282.

El-Ali, J., Gaudet, S., Gunther, A., Sorger, P. K. and Jensen, K. F. (2005). Cell stimulus and lysis in a microfluidic device with segmented gas-liquid flow. *Anal. Chem.* **77**, 3629-3636.

Esaias, W. E. and Curl, H. C. J. (1972). Effect of dinoflagellate bioluminescence on copepod ingestion rates. *Limnol. Oceanogr.* **17**, 901-906.

Fleisher, K. J. and Case, J. F. (1995). Cephalopod predation facilitated by dinoflagellate luminescence. *Biol. Bull.* **189**, 263-271.

Fogel, M. and Hastings, J. W. (1971). A substrate-binding protein in the *Gonyaulax* bioluminescence reaction. *Arch. Biochem.* **142**, 310-321.

Frangos, J. (1993). *Physical Forces and the Mammalian Cell*. San Diego: Academic Press.

Friedman, H. S. and Priebe, C. E. (1998). Estimating stimulus response latency. *J. Neurosci. Methods* **83**, 185.

Gregorio, D. E. and Pieper, R. E. (2000). Investigations of red tides along the Southern California coast. *Bull. South. Calif. Acad. Sci.* **99**, 147-160.

Groisman, A., Enzelberger, M. and Quake, S. R. (2003). Microfluidic memory and control devices. *Science* **300**, 955-958.

Gudi, S. R. P., Clark, C. B. and Frangos, J. A. (1996). Fluid flow rapidly activates G proteins in human endothelial cells. Involvement of G proteins in mechanochemical signal transduction. *Circ. Res.* **79**, 834-839.

Guillard, R. R. L. and Ryther, J. H. (1962). Studies of marine planktonic diatoms. I. *Cyclotella nana* Hustedt, and *Detonula confervacea* (Cleve) Gran. *Can. J. Microbiol.* **8**, 229-239.

Gutierrez, E. and Groisman, A. (2007). Quantitative measurements of the strength of adhesion of human neutrophils to a substratum in a microfluidic device. *Anal. Chem.* **79**, 2249-2258.

Harrison, W. G. (1976). Nitrate metabolism of the red tide dinoflagellate *Gonyaulax polyedra* Stein. *J. Exp. Mar. Biol. Ecol.* **21**, 199-209.

Hartline, D. K., Buskey, E. J. and Lenz, P. H. (1999). Rapid jumps and bioluminescence elicited by controlled hydrodynamic stimuli in a mesopelagic copepod, *Pleuromamma xiphias. Biol. Bull.* **197**, 132-143.

Hastings, J. W. and Dunlap, J. C. (1986). Cell-free components in dinoflagellate bioluminescence. The particulate activity; scintillons; the soluble components: Luciferase, luciferin, and luceferin-binding protein. *Meth. Enzymol.* **133**, 307-327.

Hobson, E. S. (1966). Visual orientation and feeding in seals and sea lions. *Nature* **210**, 326-327.

Hoy, R. R. (1989). Startle, categorical response, and attention in acoustic behavior of insects. *Annu. Rev. Neurosci.* **12**, 355-375.

Hu, W. W., Gladue, R., Hansen, J., Wojnar, C. and Chalmers, J. J. (2007). The sensitivity of the dinoflagellate *Crypthecodinium cohnii* to transient hydrodynamic forces and cell-bubble interactions. *Biotechnol. Prog.* **23**, 1355-1362.

Huh, D., Gu, W., Kamotani, Y., Grotberg, J. B. and Takayama, S. (2005). Microfluidics for flow cytometric analysis of cells and particles. *Physiological Measurement* **26**, R73-R98.

Jakobsen, H. H. (2001). Escape response of planktonic protists to fluid mechanical signals. *Mar. Ecol. Prog. Ser.* **214**, 67-78.

Jakobsen, H. H. (2002). Escape of protists in predator-generated feeding currents. *Aquatic Microbial Ecology* **26**, 271-281.

Jeong, H. J., Du Yoo, Y., Park, J. Y., Song, J. Y., Kim, S. T., Lee, S. H., Kim, K. Y. and Yih, W. H. (2005). Feeding by phototrophic red-tide dinoflagellates: five species newly revealed and six species previously known to be mixotrophic. *Aquat. Microb. Ecol.* **40**, 133-150.

Johnson, C. H., Inoe, S., Flint, A. and Hastings, J. W. (1985). Compartmentalization of algal bioluminescence: autofluorescence of bioluminescent particles in the dinoflagellate *Gonyaulax* as studied with image-intensified video microscopy and flow cytometry. *J. Cell Biol.* **100**, 1435-1446.

Juhl, A. R. (2005). Growth rates and elemental composition of *Alexandrium monilatum*, a red-tide dinoflagellate. *Harmful Algae* **4**, 287-295.

Juhl, A. R. and Latz, M. I. (2002). Mechanisms of fluid shear-induced inhibition of population growth in a red-tide dinoflagellate. *J. Phycol.* **38**, 683-694.

Juhl, A. R., Velazquez, V. and Latz, M. I. (2000). Effect of growth conditions on flow-induced inhibition of population growth of a red-tide dinoflagellate. *Limnol. Oceanogr.* **45**, 905-915.

Kamykowski, D., Reed, R. E. and Kirkpatrick, G. J. (1992). Comparison of sinking velocity, swimming velocity, rotation and path characteristics among six marine dinoflagellate species. *Mar. Biol.* **113**, 319-328.

Latz, M. I. and Jeong, H. J. (1996). Effect of red tide dinoflagellate diet and cannibalism on the bioluminescence of the heterotrophic dinoflagellates *Protoperidinium* spp. *Mar. Ecol. Prog. Ser.* **132**, 275-285.

Latz, M. I. and Lee, A. O. (1995). Spontaneous and stimulated bioluminescence in the dinoflagellate, *Ceratocorys horrida* (Peridiniales). *J. Phycol.* **31**, 120-132.

Latz, M. I. and Rohr, J. (1999). Luminescent response of the red tide dinoflagellate *Lingulodinium polyedrum* to laminar and turbulent flow. *Limnol. Oceanogr.* **44**, 1423-1435.

Latz, M. I. and Rohr, J. (2005). Glowing with the flow: ecology and applications of flow-stimulated bioluminescence. *Optics and Photonics News* **16**, 40-45.

Latz, M. I., Case, J. F. and Gran, R. L. (1994). Excitation of bioluminescence by laminar fluid shear associated with simple Couette flow. *Limnol. Oceanogr.* **39**, 1424-1439.

Latz, M. I., Juhl, A. R., Ahmed, A. M., Elghobashi, S. E. and Rohr, J. (2004a). Hydrodynamic stimulation of dinoflagellate bioluminescence: a computational and experimental study. *J. Exp. Biol.* **207**, 1941-1951.

Latz, M. I., Nauen, J. C. and Rohr, J. (2004b). Bioluminescence response of four species of dinoflagellates to fully developed pipe flow. *J. Plankton Res.* **26**, 1529-1546.

Lenz, P. H. and Hartline, D. K. (1999). Reaction times and force production during escape behavior of a calanoid copepod, *Undinula vulgaris. Mar. Biol.* **133**, 249-258.

Lenz, P. H., Hartline, D. K. and Davis, A. D. (2000). The need for speed. I. Fast reactions and myelinated axons in copepods. *J. Comp. Physiol. A* **186**, 337-345.

Levin, E. D., Chrysanthis, E., Yacisin, K. and Linney, E. (2003). Chlorpyrifos exposure of developing zebrafish: effects on survival and long-term effects on response latency and spatial discrimination. *Neurotoxicol. Teratol.* **25**, 51-57.

Lewis, J. and Hallett, R. (1997). *Lingulodinium polyedrum* (*Gonyaulax polyedra*) a blooming dinoflagellate. *Oceanogr. Mar. Biol. Ann. Rev.* **35**, 97-161.

Lu, H., Koo, L. Y., Wang, W. M., Lauffenburger, D. A., Griffith, L. G. and Jensen, K. F. (2004). Microfluidic shear devices for quantitative analysis of cell adhesion. *Anal. Chem.* **76**, 5257-5264.

Maldonado, E. M. and Latz, M. I. (2007). Shear-stress dependence of dinoflagellate bioluminescence. *Biol. Bull.* **212**, 242-249.

Mallipattu, S. K., Haidekker, M. A., Von Dassow, P., Latz, M. I. and Frangos, J. A. (2002). Evidence for shear-induced increase in membrane fluidity in the dinoflagellate *Lingulodinium polyedrum. J. Comp. Physiol. A* **188**, 409-416.

Marcos. and Stocker, R. (2006). Microorganisms in vortices: a microfluidic setup. *Limnol. Oceanogr. Methods* **4**, 392-398.

Mensinger, A. F. and Case, J. F. (1992). Dinoflagellate luminescence increases susceptibility of zooplankton to teleost predation. *Mar. Biol.* **112**, 207-210.

Morin, J. G. (1983). Coastal bioluminescence: patterns and functions. *Bull. Mar. Sci.* **33**, 787-817.

Nawata, T. and Sibaoka, T. (1979). Coupling between action potential and bioluminescence in *Noctiluca*-Effects of inorganic ions and pH in vacuolar sap. *J. Comp. Physiol. A* **134**, 137-149.

Netzel, H. and Durr, G. (1984). Dinoflagellate cell cortex. In *Dinoflagellates* (ed. D. L. Spector), pp. 43-105. Orlando, FL: Academic Press.

Nicolas, M.-T., Morse, D., Bassot, J.-M. and Hastings, J. W. (1991). Colocalization of luciferin binding protein and luciferase to the scintillons of *Gonyaulax polyedra* revealed by double immunolabeling after fast-freeze fixation. *Protoplasma* **160**, 159-166.

Preuss, T. and Faber, D. S. (2003). Central cellular mechanisms underlying temperature-dependent changes in the goldfish startle-escape behavior. *J. Neurosci.* **23**, 5617-5626.

Reinhart, W. H. (1994). Shear-dependence of endothelial functions. *Experientia* **50**, 87-93.

Rohr, J., Latz, M. I., Fallon, S., Nauen, J. C. and Hendricks, E. (1998). Experimental approaches towards interpreting dolphin-stimulated bioluminescence. *J. Exp. Biol.* **201**, 1447-1460.

Rohr, J., Hyman, M., Fallon, S. and Latz, M. I. (2002). Bioluminescence flow visualization in the ocean: an initial strategy based on laboratory experiments. *Deep Sea Res. A* **49**, 2009-2033.

Rohr, J., Schoonmaker, J., Losee, J., Latz, M. I. and Hyman, M. (1999). Flow visualization in the ocean: implications of laboratory bioluminescence experiments. In *Oceans '99 MTS/IEEE* **1**, 145-156.

Seo, K. S. and Fritz, L. (2000). Cell-wall morphology correlated with vertical migration in the non-motile marine dinoflagellate *Pyrocystis noctiluca. Mar. Biol.* **137**, 589-594.

Shankle, A. M. (2001). Population variability in the red-tide forming dinoflagellate *Prorocentrum micans*. PhD thesis, University of California San Diego, pp. 130.

Simonnet, C. and Groisman, A. (2005). Chaotic mixing in a steady flow in a microchannel. *Phys. Rev. Lett.* **94**, Art. No. 134501.

Song, J. W., Gu, W., Futai, N., Warner, K. A., Nor, J. E. and Takayama, S. (2005). Computer-controlled microcirculatory support system for endothelial cell culture and shearing. *Anal. Chem.* **77**, 3993-3999.

Spector, D. L. (1984). *Dinoflagellates.* San Diego: Academic Press.

Staples, R. F. (1966). The distribution and characteristics of surface bioluminescence in the oceans. *Naval Oceanogr. Office* **Tech. Rep. TR-184**, 1-48.

Stokes, M. D., Deane, G. B., Latz, M. I. and Rohr, J. (2004). Bioluminescence imaging of wave-induced turbulence. *J. Geophys. Res.* **109**, C01004 (8 pages).

Stone, H. A., Stroock, A. D. and Ajdari, A. (2004). Engineering flows in small devices. *Annu. Rev. Fluid Mech.* **36**, 381-411.

Stufflebeam, S. M., Poeppel, D., Rowley, H. A. and Roberts, T. P. L. (1998). Peri-threshold encoding of stimulus frequency and intensity in the M100 latency. *NeuroReport* **9**, 91-94.

Sweeney, B. M. (1986). The loss of the circadian rhythm of photosynthesis in an old strain of *Gonyaulax polyedra. Plant Physiol.* **80**, 978-981.

Swift, E. and Remsen, C. C. (1970). The cell wall of *Pyrocystis* spp. (Dinococcales). *J. Phycol.* **6**, 79-86.

Tanaka, Y., Yamato, M., Okano, T., Kitamori, T. and Sato, K. (2006). Evaluation of effects of shear stress on hepatocytes by a microchip-based system. *Meas. Sci. Technol.* **17**, 3167-3170.

Tett, P. B. (1971). The relation between dinoflagellates and the bioluminescence of sea water. *J. Mar. Biolog. Assoc. UK.* **51**, 183-206.

Vogel, S. (1981). *Life in Moving Fluids.* Princeton: Princeton University Press.

von Dassow, P. and Latz, M. I. (2002). The role of Ca^{2+} in stimulated bioluminescence of the dinoflagellate *Lingulodinium polyedrum. J. Exp. Biol.* **205**, 2971-2986.

von Dassow, P., Bearon, R. N. and Latz, M. I. (2005). Bioluminescent response of the dinoflagellate *Lingulodinium polyedrum* to developing flow: Tuning of sensitivity and the role of desensitization in controlling a defensive behavior of a planktonic cell. *Limnol. Oceanogr.* **50**, 607-619.

Weatherby, T. M., Davis, A. D., Hartline, D. K. and Lenz, P. H. (2000). The need for speed. II. Myelin in calanoid copepods. *J. Comp. Physiol. A* **186**, 347-357.

White, F. M. (1991). *Viscous Fluid Flow.* New York: McGraw-Hill.

White, H. H. (1979). Effects of dinoflagellate bioluminescence on the ingestion rates of herbivorous zooplankton. *J. Exp. Mar. Biol. Ecol.* **36**, 217-224.

Whitesides, G. M. (2006). The origins and the future of microfluidics. *Nature* **442**, 368-373.

Widder, E. A. and Case, J. F. (1981a). Bioluminescence excitation in a dinoflagellate. In *Bioluminescence Current Perspectives* (ed. K. H. Nealson), pp. 125-132. Minneapolis, Minnesota: Burgess Publishing.

Widder, E. A. and Case, J. F. (1981b). Two flash forms in the bioluminescent dinoflagellate, *Pyrocystis fusiformis. J. Comp. Physiol.* **143**, 43-52.

Wilson, T. and Hastings, J. W. (1998). Bioluminescence. *Annu. Rev. Cell Dev. Biol.* **14**, 197-230.

Wine, J. J. and Krasne, F. B. (1972). Organization of escape behavior in crayfish. *J. Exp. Biol.* **56**, 1-18.

Zhao, R., Antaki, J. F., Naik, T., Bachman, T. N., Kameneva, M. V. and Wu, Z. J. J. (2006). Microscopic investigation of erythrocyte deformation dynamics. *Biorheology* **43**, 747-765.

Zoran, M. J. and Drewes, C. D. (1988). The rapid tail withdrawal reflex of the tubificid worm *Branchiura sowerbyi. J. Exp. Biol.* **137**, 487-500.